

Mre11–Rad50–Nbs1-dependent processing of DNA breaks generates oligonucleotides that stimulate ATM activity

This is an open-access article distributed under the terms of the Creative Commons Attribution License, which permits distribution, and reproduction in any medium, provided the original author and source are credited. This license does not permit commercial exploitation or the creation of derivative works without specific permission.

Ali Jazayeri¹, Alessia Balestrini¹,
Elizabeth Garner¹, James E Haber²
and Vincenzo Costanzo^{1,*}

¹Genome Stability Unit, Clare Hall Laboratories, London Research Institute, South Mimms, Herts, UK and ²Rosenstiel Center and Department of Biology, Brandeis University, Waltham, MA, USA

DNA double-strand breaks (DSBs) can be processed by the Mre11–Rad50–Nbs1 (MRN) complex, which is essential to promote ataxia telangiectasia-mutated (ATM) activation. However, the molecular mechanisms linking MRN activity to ATM are not fully understood. Here, using *Xenopus laevis* egg extract we show that MRN-dependent processing of DSBs leads to the accumulation of short single-stranded DNA oligonucleotides (ssDNA oligos). The MRN complex isolated from the extract containing DSBs is bound to ssDNA oligos and stimulates ATM activity. Elimination of ssDNA oligos results in rapid extinction of ATM activity. Significantly, ssDNA oligos can be isolated from human cells damaged with ionizing radiation and injection of small synthetic ssDNA oligos into undamaged cells also induces ATM activation. These results suggest that MRN-dependent generation of ssDNA oligos, which constitute a unique signal of ongoing DSB repair not encountered in normal DNA metabolism, stimulates ATM activity.

The EMBO Journal (2008) 27, 1953–1962. doi:10.1038/emboj.2008.128; Published online 3 July 2008

Subject Categories: genome stability & dynamics

Keywords: ATM; DNA damage; Mre11

Introduction

Chromosomal breakage induces a robust cellular response that leads to cell cycle arrest, DNA repair, or under some circumstances, apoptosis. The ataxia telangiectasia-mutated (ATM) kinase, a member of the phosphatidylinositol 3-kinase-like kinase (PIKK) family, is central to this response (Shiloh, 2006). Essential to full ATM activation, both *in vivo* and *in vitro*, is the heterotrimeric Mre11–Rad50–Nbs1 (MRN) complex (Uziel *et al*, 2003; Costanzo *et al*, 2004a; Falck *et al*, 2005; Lee and Paull, 2005). The effect of MRN on ATM and its

activity is likely to happen on multiple levels, as well as recruitment of ATM by Nbs1 to the sites of DNA double-strand breaks (DSBs) (Falck *et al*, 2005), the MRN-dependent DSB unwinding and tethering activities are essential for efficient ATM activation (Costanzo *et al*, 2004a; Lee and Paull, 2005). MRN complex also possesses nucleolytic activity (Paull and Gellert, 1998), and interestingly, Mre11-deficient cells complemented with an Mre11 allele carrying a mutation in the nuclease catalytic site exhibit defective ATM activation (Uziel *et al*, 2003). These observations support the hypothesis that MRN nuclease activity is required for ATM activation and are consistent with the recent report showing that Mirin, an inhibitor of MRN nuclease activity, suppresses ATM activation (Dupre *et al*, 2008). The MRN complex has both exo- and endonuclease activities (Paull and Gellert, 1998). MRN endonucleolytic activity is important for DSB resection and is enhanced by CtIP (Sartori *et al*, 2007), which also has nuclease activity (Takeda *et al*, 2007). However, although MRN has a major function in DSB resection it is unclear whether this is linked to ATM activity. In budding yeast, continuous DNA resection, recruitment of DNA repair proteins and chromatin remodelling at the site of a DSB is required to maintain an active checkpoint response (Ira *et al*, 2004). This suggests that DSB processing is linked to the activation of the DNA damage response. One aspect of DSB processing that has not been investigated is that endonucleolytic processing of DSBs should lead to the generation of single-stranded DNA oligonucleotides (ssDNA oligos) as by-product. The role and the fate of these ssDNA oligos inside the nucleus are currently unknown. Recently, the presence of ssDNA oligos derived from a yet unidentified DNA-processing event has been linked to the chronic activation of the ATM-dependent DNA damage response in cells deficient for Trex1 (Yang *et al*, 2007), which is an exonuclease that degrades ssDNA to mononucleotides (Mazur and Perrino, 2001). In addition, ATM activation has been shown to require hSSB1, a novel ssDNA-binding protein (Richard *et al*, 2008). Overall, these findings suggest that ssDNA molecules have an important function in promoting and sustaining ATM activity. Here, using *Xenopus laevis* egg extract we have investigated how DNA ends are processed and how this processing influences the MRN- and ATM-dependent DNA damage response. The *Xenopus* system is ideal to study the rapid activation process of ATM following addition of DNA templates to the cell-free extract (Costanzo *et al*, 2004b). Using this approach, we found that double- and single-stranded DNA templates inducing ATM activation are extensively processed. Surprisingly, we discovered that DNA resection leads to the production of ssDNA oligos that associate with the MRN complex and influence ATM activity.

*Corresponding author. Genome Stability Unit, Clare Hall Laboratories, London Research Institute, Blanche Lane, South Mimms, Herts EN4 3LD, UK. Tel.: +44 1707 625748; Fax: +44 1707 625746; E-mail: vincenzo.costanzo@cancer.org.uk

Received: 7 February 2008; accepted: 6 June 2008; published online: 3 July 2008

Results

DNA end processing leads to formation of ssDNA oligos in *Xenopus laevis* egg extract

Synthetic DNA molecules such as annealed oligonucleotides consisting of 70 bases of random complementary sequences (rDSBs) or poly-dA₇₀/poly-dT₇₀ (pA₇₀/pT₇₀) induce ATM-dependent DNA damage response in *Xenopus* egg extract (Costanzo *et al*, 2000; Guo and Dunphy, 2000). We monitored the fate of different DNA molecules in the extract. Equal amounts of double-stranded rDSBs and pA₇₀/pT₇₀ or single-stranded pA₇₀ and pT₇₀ DNA molecules were labelled with ³²P at the 5' or 3' ends and incubated in egg extracts. DNA was then isolated and ran on sequencing gels. All DNA molecules were resected very rapidly in the extract resulting in the accumulation of mononucleotides and of ssDNA oligos ranging from 4 to 12 nucleotides in size (Figure 1A). Native gel electrophoresis of DNA derived from the extract treated with DSB molecules confirmed that these ssDNA oligos were present as single-stranded DNA as there was no difference in their molecular weight compared with denaturing gels (Supplementary Figure 1). ssDNA oligos could also be detected from internally labelled DNA, indicating that they arise from unwinding of DSBs followed by the resection of single-stranded DNA throughout its entire length (Figure 1B). Although all DNA molecules underwent resection, there were significant differences in their stability. Double-stranded DNA molecules exhibited the highest stability, whereas single-stranded DNA molecules were completely degraded after 60 min (Figure 1C). It is notable that although resection of rDSBs and pA₇₀/pT₇₀ also led to the generation of ssDNA oligos, we did not observe a reduction in the molecular weight of these DNA molecules. This is probably due the fact that nucleolytic processing is balanced by ongoing DNA repair, as in contrast to single-stranded molecules, resected double-stranded DNA molecules could undergo fill-in DNA synthesis and end joining. Indeed, the appearance of DNA molecules with higher molecular weight than rDSBs and pA₇₀/pT₇₀ confirmed this prediction (Figure 1A).

Activation of ATM by different DNA structures

Activation of ATM can be monitored by detection of serine 1981 phosphorylation (Bakkenist and Kastan, 2003), and ATM kinase activity can be measured by phosphorylation of a histone H2AX carboxy-terminal peptide containing the serine 139 (Costanzo *et al*, 2004a). We measured ATM activity triggered by different DNA molecules at increasing concentrations. rDSBs and pA₇₀/pT₇₀ induced phosphorylation of histone H2AX and ATM serine 1981 (Figure 2A and B). Surprisingly, single-stranded poly-dT₇₀ (pT₇₀) and to a much lesser extent poly-dA₇₀ (pA₇₀) induced significant ATM activity. However, circular single-stranded M13 phage DNA could not induce ATM activation even at high doses, suggesting that DNA ends are necessary for the activation of ATM (Figure 2A). In these conditions, H2AX phosphorylation is mostly dependent upon ATM as shown by the suppression of H2AX phosphorylation induced by the ATM inhibitor KU55933 (Hickson *et al*, 2004) and, to a similar extent, by ATM depletion (Supplementary Figure 2A and B). The phosphorylation status of ATM serine 1981 was consistent with H2AX phosphorylation levels and was inhibited by the ATM inhibitor (Figure 2B). ATM activation can be induced by ATR

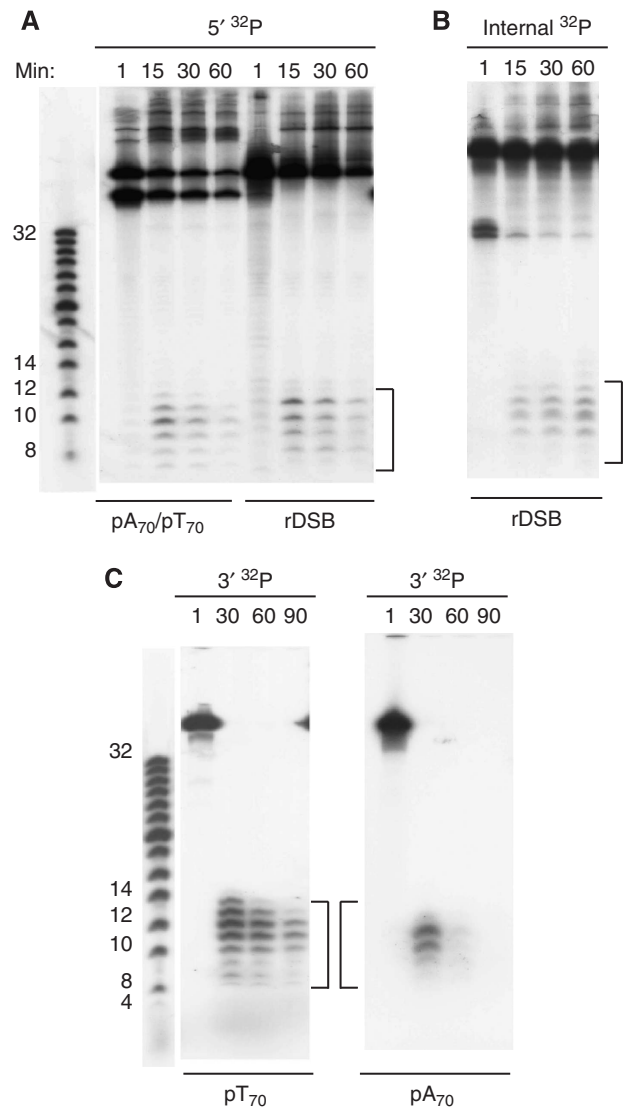


Figure 1 DNA end processing leads to generation of ssDNA oligos. (A) Different DNA structures such as rDSB and pA₇₀/pT₇₀ were stoichiometrically labelled at the 5' (5' ³²P). After incubation for the indicated times in the egg extract, the DNA was recovered and ran on a 22% denaturing acrylamide gel. In (B) rDSBs were internally labelled (internal ³²P) at the thirty-fifth nucleotide from the 5' end and in (C) pT₇₀ and pA₇₀ were labelled at the 3' end (3' ³²P) before incubation.

(Stiff *et al*, 2006). However, depletion of ATR from the egg extract did not affect the induction of ATM activation by single- and double-stranded DNA molecules, indicating that ATM was directly activated by these DNA structures (Supplementary Figure 3A and B). pT₇₀-induced ATM activation might be due to the conversion of single-stranded pT₇₀ into double-stranded DNA in the extract. To rule out this possibility, we monitored pT₇₀ replication at different concentrations. We observed efficient pT₇₀ replication at concentrations higher than the ones already capable of inducing ATM activation (Supplementary Figure 4). This indicated that pT₇₀ molecules were able to induce ATM activation in the single-stranded form. pT₇₀ replication at high doses might be due to the saturation of the enzymes responsible for pT₇₀ degradation resulting in subsequent stabilization of a fraction of pT₇₀ molecules, which then become available to the single-

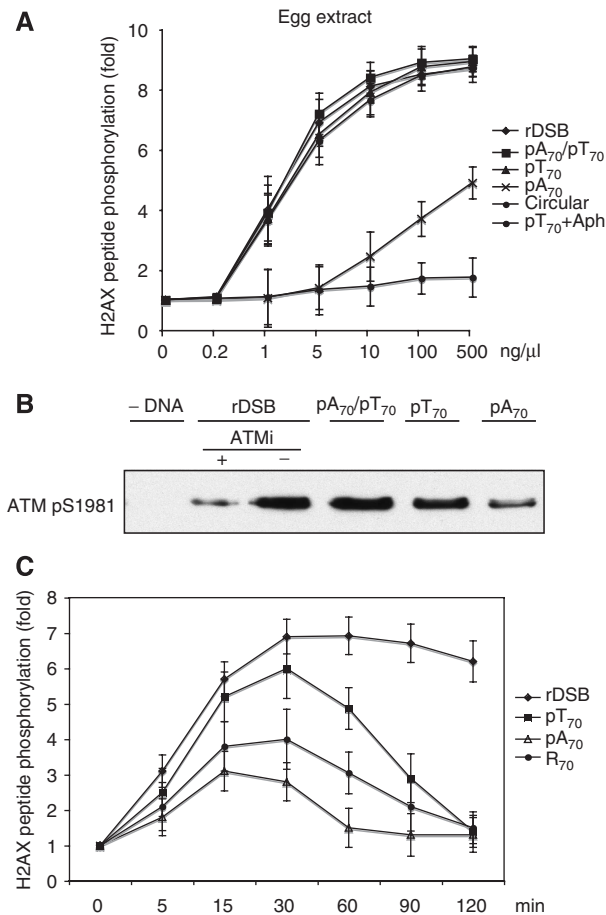


Figure 2 ATM activation by different DNA structures. (A) Histone H2AX carboxy-terminal peptide phosphorylation in the presence of increasing amounts of rDSB, pA₇₀/pT₇₀, pT₇₀, pA₇₀, M13 circular ssDNA or pT₇₀ plus 100 μM aphidicolin (Aph). Activity was measured 15 min after incubation of DNA in the extract at 22°C and is expressed as fold induction over the activity measured in the untreated extract. (B) ATM serine 1981 phosphorylation in the untreated (-DNA) egg extract or extract supplemented with rDSB in the absence or presence of 10 μM Ku55933 (ATMi), 2.5 ng/μl pA₇₀/pT₇₀, pT₇₀ or pA₇₀ or after 30 min of incubation. Western blot was performed with Advance ECL for enhanced sensitivity. (C) Histone H2AX peptide phosphorylation in the presence of egg extract containing no DNA, 2.5 ng/μl rDSB, pT₇₀ or 25 ng/μl pA₇₀ and R₇₀ measured at the indicated time points after DNA addition. Activity is expressed as fold induction. In all graphs, the values are average of three independent experiments and the error bars represent standard deviation.

stranded DNA replication machinery. Replicated pT₇₀ molecules contribute to the induction of DNA damage response to DSBs in the egg extract as previously shown (Guo and Dunphy, 2000). We also measured ATM activity in response to low concentration of pT₇₀ in the presence of high amounts of aphidicolin, which inhibits DNA polymerases and single-stranded DNA synthesis in the egg extract (Jenkins *et al*, 1992). As shown in Figure 2A, ATM activation by pT₇₀ is refractory to aphidicolin treatment. Activation of ATM by pT₇₀ was also observed after gel purification of pT₇₀ oligos and was suppressed by pretreating pT₇₀ oligos with DNase, confirming that it was not due to contaminants of pT₇₀ synthesis (data not shown). These data suggest that double as well as some single-stranded linear DNA molecules can stimulate ATM activity.

ssDNA oligos and ATM activity

We then correlated the stability of DNA templates to the persistence of ATM activity. To this end, rDSBs, pA₇₀, pT₇₀ and single-stranded DNA molecules with random DNA sequence (R₇₀) were incubated in the egg extract. ATM activity was monitored at various time points from DNA addition. Incubation of rDSBs, pT₇₀, R₇₀ and to a lesser extent of pA₇₀ molecules in the extract resulted in stimulation of ATM activity (Figure 2C). Significantly, ATM activity reached its peak and was maintained at time points when most of the single-stranded DNA templates such as pT₇₀ and pA₇₀ were degraded into smaller ssDNA oligos (Figures 1C and 2C). Further degradation of ssDNA oligos to mononucleotides correlated instead with the complete loss of ATM activity. In contrast, no significant loss of ATM activity was observed with rDSB molecules, whose stability was not affected over time (Figures 1C and 2C). ssDNA oligos derived from pA₇₀, which, compared with pT₇₀-derived ssDNA oligos were more rapidly degraded to mononucleotides, were less effective at promoting sustained ATM activity (Figure 2C). To further probe the role of ssDNA oligos, we measured H2AX phosphorylation after the removal of pA₇₀/pT₇₀ from the extract. To this end, biotinylated pA₇₀/pT₇₀ oligos were incubated in the extract and removed after 30 min with streptavidin beads (Figure 3A). To verify that ssDNA oligos had been generated from pA₇₀/pT₇₀ before its removal, we labelled pA₇₀/pT₇₀ on the 3' end of the DNA complementary to the biotinylated strand. After 30 min of incubation in the extract, ssDNA oligos were generated from pA₇₀/pT₇₀ processing and could not be eliminated by the removal of biotinylated pA₇₀/pT₇₀ (Figure 3B). ATM activity was then measured in the pA₇₀/pT₇₀-depleted extracts. Consistent with previous observations (Dupre *et al*, 2006), removal of pA₇₀/pT₇₀ did not affect ATM activity, indicating that once the signal has been initiated the kinase is able to maintain its activity even in the absence of pA₇₀/pT₇₀. To demonstrate a role for ssDNA oligos in maintaining ATM activity, we tested different nucleases for their ability to eliminate ssDNA oligos. We found that phosphodiesterase I (PDEI), which is known to preferentially degrade single-stranded DNA to mononucleotides as terminal products (Razzell and Khorana, 1959a, b), was able to efficiently degrade small ssDNA oligos in the egg extract (Figure 3B) and to suppress ATM activity after removal of pA₇₀/pT₇₀ (Figure 3C). Although PDEI could also degrade RNA or poly-ADP ribose polymers (PARP), we found no effect of RNA degradation or PARP synthesis inhibition on ATM activity (Supplementary Figure 5). Importantly, we could demonstrate that PDEI in the conditions used for these experiments specifically degraded small ssDNA oligos and not larger double-stranded DNA molecules (Supplementary Figure 6). Taken together, these results indicate that the ssDNA oligos generated from linear DNA processing sustain ATM activity.

The MRN complex mediates the effects of ssDNA oligos on ATM activity

As ATM activation requires the MRN complex in *Xenopus* egg extract at low doses of DSBs (Costanzo *et al*, 2004a; Dupre *et al*, 2006), we were intrigued to know whether the MRN complex was promoting ATM activity induced by ssDNA oligos. Biotinylated pA₇₀/pT₇₀ molecules were incubated in the extract for 30 min and then removed. The MRN complex

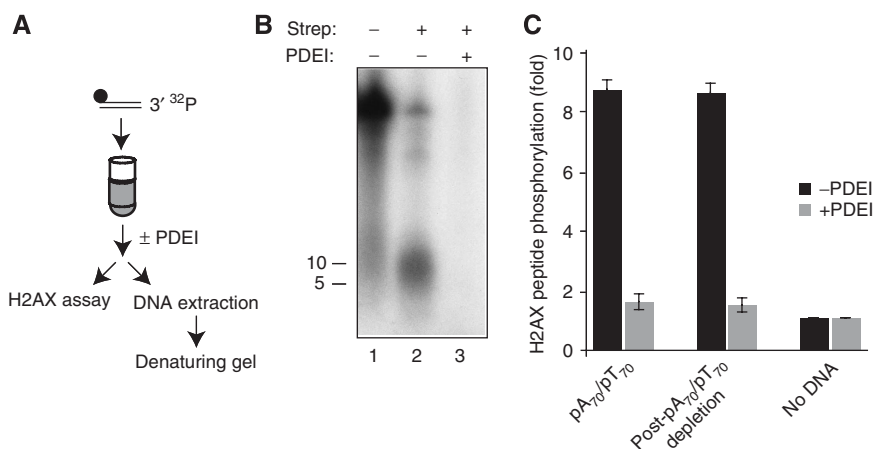


Figure 3 ssDNA oligos sustain ATM activity. **(A)** Experimental procedure: biotinylated pA₇₀/pT₇₀ labelled with ³²P on the 3' end was incubated for 30 min in the extract and then removed with streptavidin beads. After pA₇₀/pT₇₀ removal, histone H2AX peptide phosphorylation was monitored. **(B)** Residual DNA left in the extract was isolated and run on a 15% TBE-urea denaturing gel. DNA was isolated from the extract incubated with biotinylated and labelled pA₇₀/pT₇₀ for 30 min (lane 1) and from extracts in which biotinylated pA₇₀/pT₇₀ was incubated for 30 min and then removed with streptavidin beads (Strep) (lanes 2 and 3). The extracts were untreated (lane 2) or supplemented with 0.001 U/μl PDEI (lane 3). **(C)** Histone H2AX peptide phosphorylation induced by 5 ng/μl biotinylated pA₇₀/pT₇₀ before and after pA₇₀/pT₇₀ removal in the absence (black bar) or in the presence (grey bar) of 0.001 U/μl PDEI. PDEI was added 30 min after DNA addition and was incubated for 10 min at 22°C. Activity is expressed as fold induction over the untreated extract (no DNA).

was subsequently immunoprecipitated from the extract with polyclonal antibodies raised against Mre11 (Costanzo *et al*, 2004a; Dupre *et al*, 2006). Depletion of the MRN complex led to the loss of ATM activity, suggesting that it was required to sustain ATM activity (Figure 4A). As the MRN complex tethers DNA fragments resulting in an increase in the local concentration of ATM and DNA ends (Costanzo *et al*, 2004a; Dupre *et al*, 2006), we postulated that the MRN complex might bind to ssDNA oligos. To test this possibility, biotinylated pA₇₀/pT₇₀ labelled with ³²P at the 3' end was incubated in the egg extract for 30 min and then removed. Following immunoprecipitation of Mre11, we could detect the presence of ³²P-labelled ssDNA oligos in the immunoprecipitated samples (Figure 4B). Treatment of the immunoprecipitated Mre11 with PDEI led to degradation of labelled ssDNA oligos (Figure 4B). To verify whether the MRN-ssDNA oligos complexes were able to stimulate ATM activity, we incubated immunoprecipitated Mre11 derived from pA₇₀/pT₇₀-treated extracts in fresh extracts containing pA₇₀/pT₇₀ or rDSB at concentrations not sufficient to induce ATM activation. The presence of high molecular weight DNA facilitated the formation of DNA-protein complexes with increased local concentration of MRN and ATM molecules as previously shown (Costanzo *et al*, 2004a; Dupre *et al*, 2006). In this case, the MRN-ssDNA oligos complexes led to partial activation of ATM activity (Figure 4C). Significantly, MRN-ssDNA oligos complexes pretreated with PDEI, which was then washed away, were unable to induce ATM activation, suggesting that ssDNA oligos associated with MRN were active intermediates capable of promoting ATM activity (Figure 4C). To further confirm the role of ssDNA oligos in ATM activation, we incubated synthetic poly-dT₅ (pT₅) and poly-dT₁₀ (pT₁₀) oligonucleotides in the extract and measured ATM activity. However, these synthetic oligonucleotides failed to activate ATM in the extract (data not shown). This was likely due to the rapid degradation of exogenous pT₅ and pT₁₀ oligonucleotides in the egg cytoplasm (Supplementary Figure 7). ssDNA oligos generated from processed ends were instead stable for

more than 60 min (Figure 2A), suggesting that ssDNA oligos are stabilized by the rapid association with protein complexes such as MRN immediately after their generation. Notably, ssDNA oligos did not interfere with the ability of the MRN complex to promote end-to-end bridging of linear double-stranded DNA molecules (Supplementary Figure 8), indicating that ssDNA oligos interact with parts of the MRN complex that are not involved in DNA tethering.

ssDNA oligos formation from chromosomal DSBs is MRN dependent

To show that ssDNA oligos generation is a physiologically relevant phenomenon, we sought to establish whether ssDNA oligos could be generated following induction of chromosomal breakage. Strikingly, *EcoRI* treatment of sperm nuclei induced the accumulation of ssDNA oligos that were efficiently degraded by PDEI (Figure 5A). ssDNA oligo formation over time was impaired by depletion of the MRN complex and restored by supplementing the egg extract with recombinant human MRN complex (Figure 5B). This indicates that ssDNA oligo generation is due to MRN-dependent processing of DNA ends produced by *EcoRI*. The fact that human MRN complex restored the formation of ssDNA oligos in the egg extract confirmed that the ability to promote DSB processing is a conserved feature of the MRN complex. *EcoRI*-dependent chromosomal breakage induced ATM activation in the egg extract as previously reported (Yoo *et al*, 2004). Consistent with the data obtained with synthetic DNA templates, the degradation of ssDNA oligos by PDEI also led to the suppression of ATM activation (Figure 5C) induced by chromosomal breakage. Importantly, ATM activation by *EcoRI*-induced breaks was MRN dependent as it was abolished in Mre11-depleted extract (Figure 5D).

ssDNA oligos induce ATM activation in human cells

To demonstrate that generation of ssDNA oligos at chromosomal breaks is a conserved phenomenon, we developed a protocol to isolate DNA oligos from human cells after

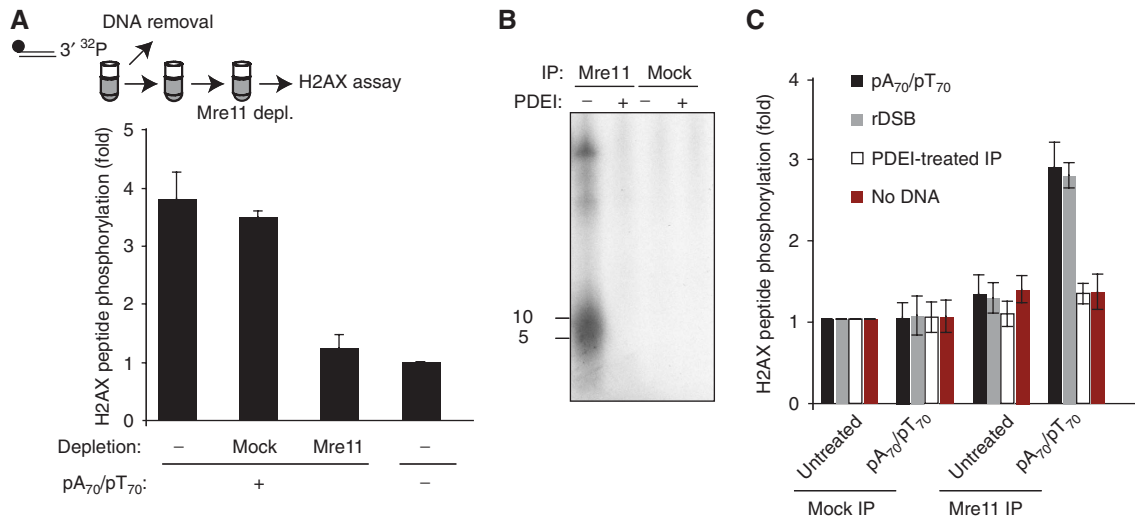


Figure 4 ssDNA oligos form DNA-protein complexes with MRN that are able to induce ATM activation. (A) Biotinylated labelled pA₇₀/pT₇₀ was incubated in the extract for 30 min and following DNA removal with streptavidin beads, Mre11 was depleted and ATM activity was monitored. Activity is expressed as fold induction over the untreated samples. (B) ³²P-labelled DNA isolated from Mre11 or mock immunoprecipitations was run on a 15% TBE-urea denaturing gel. Immunoprecipitates were untreated or treated with 0.001 U/μl PDEI. (C) Histone H2AX peptide phosphorylation induced by Mre11 immunoprecipitated from an untreated or a pA₇₀/pT₇₀-treated extract and transferred to an extract supplemented with low concentrations of pA₇₀/pT₇₀ (0.2 ng/μl) (black bar), rDSB (0.2 ng/μl) (grey bar) or no DNA (red bar). Immunoprecipitates were also treated with 0.001 U/μl PDEI for 10 min at 22°C before transfer into the extract supplemented with low concentrations of DNA (white bar).

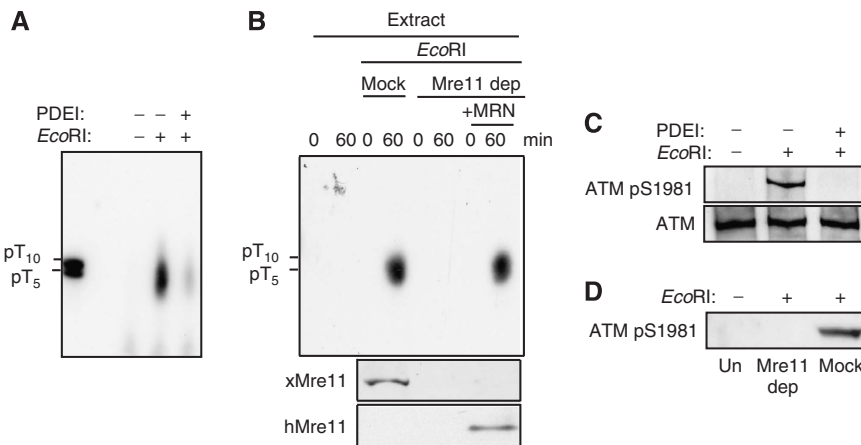


Figure 5 ssDNA oligos are generated from MRN-dependent processing of chromosomal DSBs. (A) Sperm nuclei were incubated in the extract for 30 min. The extract was then supplemented with 0.2 U/μl of *Eco*RI in the presence or absence of 0.001 U/μl of PDEI and the samples were incubated for a further 60 min. Sperm nuclei were permeabilized and processed to isolate soluble low molecular weight DNA. DNA was labelled with TdT in the presence of ³²P-alpha-ddATP and ran on a 15% TBE-urea denaturing gel. (B) Upper panel: sperm nuclei were incubated in the extract for 30 min, after which the extract was supplemented with 0.2 U/μl *Eco*RI and immediately processed to isolate low molecular weight DNA (0 min) or incubated for a further 60 min. The extracts were untreated, mock depleted (mock) or Mre11-depleted (Mre11 dep) and supplemented with recombinant MRN complex (+MRN) (250 nM). Lower panels: egg extract treated as indicated in the upper panel was probed with anti-*Xenopus* (xMre11) and anti-human Mre11 (hMre11) antibodies. (C) Sperm nuclei were incubated in the extract in the presence or absence of 0.2 U/μl of *Eco*RI or 0.001 U/μl of PDEI for 60 min. ATM was immunoprecipitated and immunoblotted as indicated. (D) Sperm nuclei were incubated in the extracts that were untreated (Un), mock depleted (mock) or Mre11 depleted (Mre11 dep) in the presence or absence of 0.2 U/μl of *Eco*RI for 60 min. ATM was immunoprecipitated and immunoblotted as indicated.

induction of DSBs. Using this protocol, we could isolate ssDNA oligos from human U2OS cells treated with ionizing radiation (IR) (Figure 6A). ssDNA oligos were also isolated from G1-arrested cells, suggesting that ssDNA oligo production as ATM activation is not restricted to S phase (Supplementary Figure 9). We then tested the effect of ssDNA oligos on ATM in mammalian cells. To this end, we microinjected pT₅ oligonucleotides into human U2OS cells. This procedure allowed reaching a high nuclear concentration of ssDNA oligos overcoming ssDNA degradation that

usually occurred with alternative methods based on liposome-mediated transfer (data not shown). To identify the injected cells, we used anti-goat IgG conjugated with Alexa Fluoro 488 as injection marker. ATM activation in the injected cells was monitored by detecting ATM phospho-serine 1981 (pSerine 1981). The DNA-injection marker mixture was injected in proximity to the nuclear periphery. Microinjection of cells with pT₅ led to activation of ATM in the injected cells (Figure 6B). This response was completely inhibited when cells were pre-incubated with the ATM

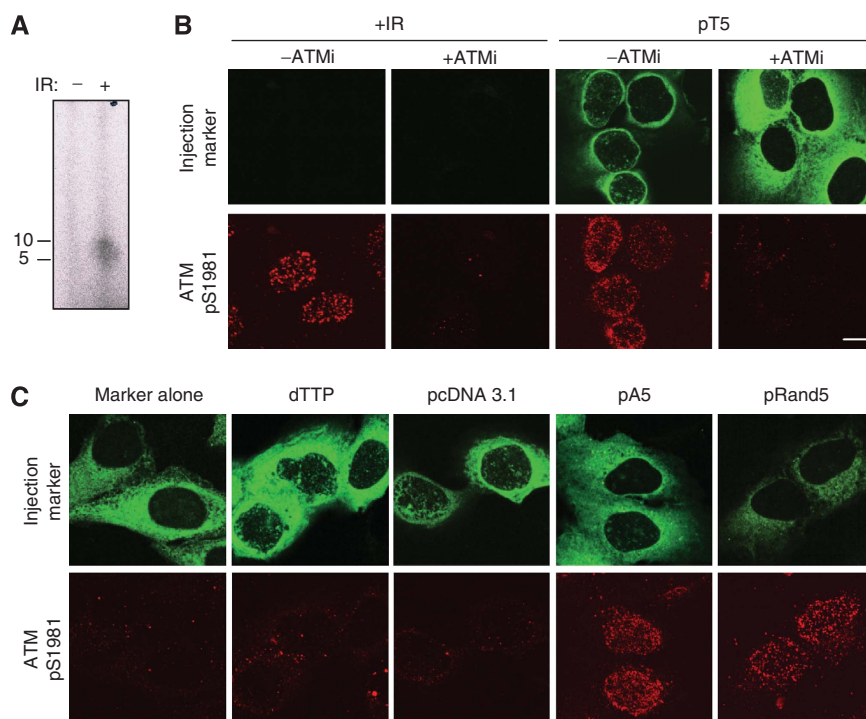


Figure 6 ssDNA oligos are generated following induction of DSBs in human cells and promote ATM activation when injected in undamaged cells. **(A)** Human U2OS cells were irradiated with 10 Gy of IR. Following a short recovery, cells were permeabilized and processed to isolate soluble low molecular weight DNA. DNA was labelled with TdT in the presence of ^{32}P -alpha-ddATP and ran on a 15% TBE-urea denaturing gel. **(B)** U2OS cells were co-microinjected with $5\ \mu\text{g}/\mu\text{l}$ pT₅ and anti-goat IgG conjugated with Alexa Fluor 488. After 30 min incubation, cells were fixed and stained with anti-ATM phospho-serine 1981 antibody. Where indicated cells were treated with 10 Gy of IR and after 1 h were fixed and immunostained. The ATM inhibitor (ATMi) was used at $10\ \mu\text{M}$ for 1 h prior to irradiation or microinjection. **(C)** U2OS cells were injected as indicated. All DNA concentrations were at $5\ \mu\text{g}/\mu\text{l}$ and dTTP was $100\ \mu\text{M}$. After 30 min incubation, cells were fixed and stained with anti-ATM phospho-serine 1981 antibody. All the images were acquired under identical microscope settings. Scale bar is 10 mm.

inhibitor KU55933 (Figure 6B). Furthermore, microinjection of pA₅ or a mixture of random 5-mers also led to ATM activation (Figure 6C). Injecting cells with the injection marker alone, dTTP or circular DNA did not lead to detectable ATM activation (Figure 6C). ATM activation by small ssDNA oligos was observed in the majority of the injected cells (Supplementary Figure 10A). Quantification of the immunofluorescence intensity obtained with anti-phospho-ATM also revealed a robust activation of ATM induced by ssDNA oligos in the injected cells (Supplementary Figure 10B). ATM activation was detected immediately after oligo injection to exclude the interference of ssDNA oligos with DNA metabolic processes such as DNA replication or transcription. ssDNA oligos-induced ATM activation resulted in small and diffuse foci (Figure 6B and C) that were different from the large DNA damage foci typical of chromosomal breakage induced by IR (Figure 6B). The absence of genomic DSBs in cells injected with various ssDNA oligos was confirmed by the absence of DNA damage foci containing phosphorylated histone H2AX (Supplementary Figure 11).

Discussion

MRN-dependent ssDNA oligo generation at DSBs

Here, we have shown that DNA molecules with free DNA ends triggering ATM activation are rapidly processed resulting in the generation of ssDNA oligos. These molecules are not simple by-products of DNA resection as they participate in the ATM-dependent DNA damage response. We have

demonstrated that generation of ssDNA oligos from chromosome breaks requires the MRN complex. In addition, we have shown that the MRN complex bound to ssDNA oligos promotes ATM activity, indicating that ssDNA oligos function as allosteric cofactors activating the complex. It is known that the MRN complex containing nuclease-inactive Mre11 fails to promote ATM activation (Uziel *et al*, 2003). In addition, Mirin, a chemical that inhibits Mre11 nuclease activity without affecting MRN and ATM binding to DSBs, suppresses ATM activity (Dupre *et al*, 2008). Our findings are consistent with the requirement for the MRN complex nuclease activity in the ATM activation process. Once ssDNA oligos have been generated, they remain associated with the MRN complex and probably promote a stable conformation capable of inducing continuous stimulation of ATM molecules. This process, likely, requires the generation of a limited amount of ssDNA oligos bound to MRN complex and does not require extensive resection to activate a large number of ATM molecules. This model is compatible with the lack of extensive resection in G1-arrested cells in which ATM can be activated (Jazayeri *et al*, 2006; Sartori *et al*, 2007). In addition, we show that ssDNA oligo formation can take place also in G1-arrested cells after treatment with IR. This is consistent with the recently reported resection of 'ragged' DNA ends induced by IR in G1-arrested cells (Barlow *et al*, 2008). ssDNA oligos produced at DSBs could interact with one or more subunits of the MRN complex that have DNA-binding domains. The binding of dinucleoside polyphosphates to the MRN complex through the Rad50 subunit has recently been demonstrated

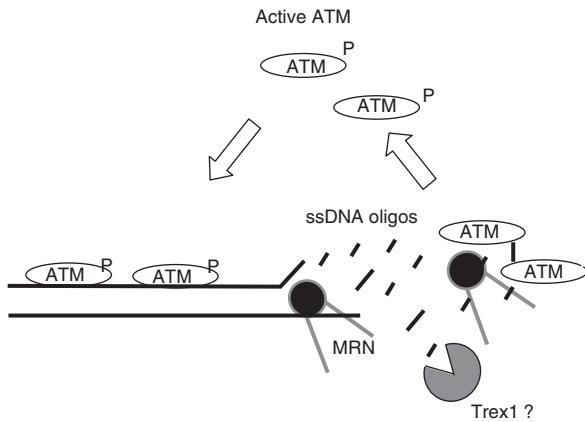


Figure 7 Proposed model for ssDNA oligo action. ssDNA oligos generated by MRN-dependent processing of DSBs stimulates ATM activity by forming MRN–DNA oligo complexes. Elimination of ssDNA oligos by single-stranded DNA exonucleases such as Trex1 (see Discussion) might indirectly control ATM activity.

and suggests that the activities of the MRN complex are regulated by different nucleotide metabolites (Bhaskara *et al*, 2007).

Alternatively, it is also possible that the MRN complex is not the only mediator of ssDNA oligos' effect on ATM. ssDNA oligos might also influence ATM activity binding other targets such as the recently discovered ssDNA-binding protein hSSB1, which has high affinity for small ssDNA oligos and is required for ATM activation (Richard *et al*, 2008). Overall, these observations are consistent with reports showing the existence of a multiple step activation mode of ATM (Dupre *et al*, 2006; Berkovich *et al*, 2007) and suggest that ssDNA can trigger an initial activation of ATM, which can be amplified and maintained by ssDNA oligos generation. ssDNA oligos may increase the activity of ATM molecules already bound to DSBs or facilitate the activation of inactive ATM molecules that have not yet engaged DSBs (Figure 7). However, the absence of ATM-dependent phosphorylation of histone H2AX triggered by ssDNA oligos alone suggests that ssDNA oligos are not sufficient to enable ATM-dependent phosphorylation of chromatin-bound targets. This event probably requires the presence of double-stranded DNA ends onto which ATM can load. This is also suggested by the fact that, differently from linear DNA, single-stranded circular DNA is unable to trigger any ATM activity.

As far as the mechanism of ssDNA oligo generation is concerned, the detection of ssDNA oligos from internally labelled DNA indicates that they are produced by the combined actions of endo- and exonuclease activities described for the MRN complex. The MRN complex might exert an effect on single-stranded DNA generated by helicase-mediated unwinding of DSBs. Interestingly, we found that generation of ssDNA oligos from chromosomal DSBs is entirely dependent upon MRN, whereas small amounts of ssDNA oligos generated from synthetic DNA templates can still be detected in the absence of MRN (data not shown). This indicates that MRN complex activity is specific for DSB processing that arise in the context of the chromatin, consistent with its chromatin-remodelling activities (Tsukuda *et al*, 2005).

ssDNA oligos turnover is linked to ATM activation status

An important aspect of ssDNA oligo metabolism is their turnover as the persistence of ssDNA oligos is correlated with the activation status of ATM. We showed that in *Xenopus* egg extract, exogenous synthetic small ssDNA oligos are rapidly degraded, whereas ssDNA oligos derived from the resection of larger DNA templates are more stable. This is likely due to their association with factors involved in DNA resection such as the MRN complex or other ssDNA-binding proteins. Interestingly, the ssDNA-binding protein hSSB1, which is highly conserved in *Xenopus*, has a higher binding affinity for poly-pyrimidine than for poly-purine containing ssDNA molecules (Richard *et al*, 2008). The association of ssDNA oligos to proteins such as hSSB1, if proven, might explain the higher intrinsic stability and efficiency at stimulating ATM activity of poly-pyrimidine pT₇₀ compared with poly-purine pA₇₀ oligos in the egg extract.

Predictably, the elimination of ssDNA oligos would be required for efficient inactivation of ATM once DSBs have been repaired, whereas the persistence of ssDNA oligos would maintain ATM active. ssDNA oligos elimination could be mediated by an exonuclease capable of degrading ssDNA oligos. Among known nucleases, Trex1, which has an activity similar to PDE1, can degrade ssDNA oligos (Mazur and Perrino, 2001). Mutations in Trex1 are responsible for the Aicardi–Goutieres syndrome, a complex human disease that recapitulates the effects of an embryonic response to a viral DNA infection (Crow *et al*, 2006). The deficiency of Trex1 activity leads to the accumulation of free ssDNA oligos and this correlates with chronic stimulation of the ATM-dependent DNA damage response (Yang *et al*, 2007). Therefore, Trex1 is an ideal candidate for the regulation of ssDNA oligos stability and, indirectly, ATM activity (Figure 7). Interestingly, Trex1 is confined to endoplasmic vesicles and ssDNA oligos need to be exported from nuclei for degradation (Yang *et al*, 2007). In our experiments, direct injection of ssDNA oligos into cells bypasses this degradation pathway reaching a nuclear concentration able to stimulate ATM. Taken together, these findings indicate an important and unexpected role for the ssDNA oligos metabolism in the DNA damage response.

ssDNA oligos as an alarm signal

The creation of ssDNA oligos during the resection of DNA undergoing repair, either from 5' to 3' processing of DSBs or possibly from enlarging gaps in other forms of DNA repair is a unique signal of DNA damage. Whereas mononucleotides are produced by normal DNA metabolism, these ssDNA oligos are only present when DNA damage is being processed. ssDNA oligos could function as an alarm signal that promotes full activation of the DNA damage response. Thus, whereas DSB ends and ssDNA are necessary to establish a platform to assemble factors required for the localized activation of the checkpoint and for the repair of the damage, a widespread and efficient DNA damage response—which should be turned off when repair is complete—takes advantage of DNA species that are only produced while repair is ongoing. The fact that single-stranded circular DNA, which is not degraded, is unable to trigger sustained ATM activation is consistent with the hypothesis that ssDNA in the absence of DNA processing is not sufficient to activate ATM. In budding yeast, where repair can be carefully monitored,

resection continues at a rate of 4 kb/h from DSB ends for as long as it takes the process of repair to be completed, and the checkpoint is turned off soon after repair is complete (Vaze *et al*, 2002; Keogh *et al*, 2006). In the absence of yeast Mre11, the DNA damage checkpoint is initiated, but not maintained as in wild-type cells (Lee *et al*, 1998; D'Amours and Jackson, 2001), indicating a role for Mre11 in sustaining the checkpoint. Importantly, ssDNA oligos can also be observed following induction of DSBs in human cells, indicating that this is a conserved physiological phenomenon. The introduction of ssDNA oligos in cancer cells could be therapeutically exploited to enhance DNA damage response without producing further damage to the genome.

Materials and methods

Xenopus egg extract

The egg extracts were prepared as previously described (Costanzo *et al*, 2004a). Interphase extract was obtained by releasing CSF-arrested extract with 0.4 mM CaCl₂.

DNA structures

All DNA oligos were obtained from Sigma-Genosys. Random 70 mer complementary single-stranded DNA molecules (rDSB) had the following sequence:

5'-TGGGTCTCTCTGGGCTTCTGGTCTCTGGACAACAGATCAAGG
CAACCATGGCCACACACTCAAGGGC-3'

5'-GCCCTTGAGTGTGGGCCATGGTGCCTTGATCTGTTGTCCA
GGAGACCAGAAGCCAGAGACCCA-3'

Equimolar amounts of single-stranded DNA oligos were annealed in a buffer containing 10 mM HEPES (pH 7.5) and 5 mM MgCl₂ at 95°C for 1 min, 65°C for 10 min, 37°C for 10 min and 22°C for 10 min in a PCR Thermocycler to obtain double-stranded DNA poly-dA₇₀/dT₇₀ and rDSB. Biotinylated poly-dA₇₀/dT₇₀ was obtained by annealing 3'-biotinylated poly-dT₇₀ to poly-dA₇₀. DNA concentration was measured in the Nanodrop spectrophotometer.

H2AX kinase assay

Interphase egg extracts were incubated with DNA structures as indicated at 22°C. The extract (2 µl) was mixed with 20 µl of EB kinase buffer (20 mM HEPES (pH 7.5), 50 mM NaCl, 10 mM MgCl₂, 1 mM DTT and 10 mM MnCl₂) supplemented with 0.5 mg/ml histone H2AX peptide (Sigma-Genosys), 50 µM ATP and 10 µCi of g-³²P-ATP 10 µCi/µl (greater than 3000 Ci/mmol). The samples were incubated at 30°C for 5 min, and reactions were spotted on p81 phosphocellulose filter paper (Upstate Biotechnology). Filters were air-dried and washed three times in 5% phosphoric acid. Radioactivity was quantified in a scintillation counter. PARP inhibitor was obtained from BIOMOL and RNaseA from Qiagen. The extract used to measure H2AX phosphorylation was pre-incubated twice for 20 min at 4°C with a volume of streptavidin-coated beads (Dynal) coupled to 5' biotinylated double-stranded 20 mer oligos (with a sequence corresponding to the first 20 nucleotides of rDSB oligos) that were then removed to eliminate H2AX kinase activity due to DNA-PK (Dupre *et al*, 2006).

DNA labelling

Poly-dA₇₀/dT₇₀ poly-dA₇₀, poly-dT₇₀ and rDSB were labelled at the 5' end using T4 polynucleotide kinase. Briefly, 10 ng of DNA was incubated with 30 U T4 kinase (NEB) for 4 h at 37°C in 30 µl reaction in the T4 kinase buffer (NEB) in the presence of 10 µCi of g-³²P-ATP 10 µCi/µl (greater than 3000 Ci/mmol). Excess of enzyme and long incubation time ensured stoichiometric labelling of the DNA. Poly-dA₇₀/dT₇₀ poly-dA₇₀, poly-dT₇₀ and rDSB 3' end labelling was done by incubating 10 ng of DNA with 20 U TdT (Fermentas) for 4 h at 37°C in 30 µl reaction in the presence of TdT reaction buffer (Fermentas) and 10 µCi of alpha-³²P-ddATP 10 µCi/µl (greater than 3000 Ci/mmol). Labelled DNA was purified through G25 gel filtration columns (Amersham). DNA concentration was measured in the Nanodrop spectrophotometer. ³²P-labelled poly-dA₇₀/dT₇₀ was obtained by annealing 3'-³²P-labelled poly-dT₇₀ to poly-dA₇₀. ³²P-labelled biotinylated poly-dA₇₀/dT₇₀ was obtained by annealing 3'-biotinylated poly-dA₇₀ to 3'-³²P-labelled poly-dT₇₀. For internally

labelled oligos, a 35-mer oligo (5'-TGCTGACCTTGTTTTGGGA CGTCTACTCATCTC-3') was ³²P labelled at the 5' end with T4 polynucleotide kinase. The labelled oligo was annealed to a 70-mer oligo (5'-GAGATGAGTAGACGTCCCAAAAACAAGGTCAGACATCGTG ACACATTCTGTCCGGTCTAGGGCATGGATG-3') to generate a double-stranded oligo with a 35-mer overhang. This structure was then annealed to another 35-mer oligo (5'-CATCCATGCCCTAGACCGGA CAGATGTGTACCA-3'), complementary to the overhang region, followed by a ligase reaction to join the two adjacent 35-mer oligos. The excess ssDNA in the reaction was removed with *ExoI* treatment. Labelled DNA was purified through G25 gel filtration columns (Amersham).

DNA-processing reaction

Poly-dA₇₀/dT₇₀, poly-dA₇₀, poly-dT₇₀ or rDSB labelled at the 5' or 3' end was mixed with 10 µl of the egg extract and incubated at 22°C for 0, 1, 30, 60 and 90 min. Reactions were stopped with 40 µl stop buffer (0.5% SDS, 80 mM Tris pH 8.0 and EDTA 8 mM). Here, 10 µl of the reaction was mixed with Tris-urea denaturing loading buffer (Invitrogen), heated at 70°C for 3 min and run on 22% Tris-urea acrylamide sequencing gel using a Bio-Rad apparatus. Alternatively, 15% TBE-urea acrylamide or TBE-acrylamide pre-cast gels from Invitrogen were used. Oligonucleotide DNA marker (Amersham) used was labelled with TdT as described above. Gels were washed in a fixative (35% MeOH, 18% acetic acid) for 30 s, wrapped in saran-wrap and immediately exposed. Purified 5'-nucleotide-free PDEI derived from *Crotalus adamanteus* venom (Sigma-Genosys) was a gift from T Lindhal. The enzyme was typically used at 0.001–0.002 U/µl.

ATM, ATR and Mre11 depletions and western blots

For Mre11, ATM and ATR depletions, 100 µl of interphase extracts was incubated with 50 µl protein A Sepharose beads coupled to 100 µl of anti-X-Mre11, anti-X-ATM or anti-X-ATR serum for 45 min at 4°C twice. For mock depletion, protein A Sepharose beads washed in PBS were used. Mre11 antibodies and production of recombinant histidine-tagged MRN complex have been previously described (Costanzo *et al*, 2004a). Anti-human Mre11 antibodies were from Bethyl. Anti-X-ATM and anti-X-ATR polyclonal antibodies were previously described (Trenz *et al*, 2006). Detection of ATM pSerine 1981 by western blot was obtained with mouse anti-ATM pSerine 1981 (Rockland Immunochemicals) overnight in blocking solution using Advanced ECL (Amersham).

Isolation of DNA oligonucleotides

DNA oligonucleotides associated with Mre11 immunoprecipitates were detected as following: 100 ng poly-dA₇₀/dT₇₀ was ³²P-labelled at 3' end of the poly-dT₇₀ using TdT as described above. The reaction was scaled up by a factor of 10. ³²P-labelled poly-dA₇₀/dT₇₀ (100 ng) was incubated in 100 µl egg extracts for 30 min. Protein A Sepharose beads (50 µl) coupled to 100 µl of anti-X-Mre11 serum were then added to the extracts. For mock depletions, protein A Sepharose beads washed in PBS were used. Reactions were incubated for 45 min at 22°C. Sepharose beads were then isolated by 1 min centrifugation at 1000 r.p.m. at 4°C and washed three times with PBS supplement with 0.4% NP40. The samples were resuspended in TBE-urea loading buffer (Invitrogen), heated at 70°C for 3 min and run on a 15% TBE-urea acrylamide pre-cast gels (Invitrogen).

DNA oligonucleotides accumulated in response to *EcoRI* treatment were isolated as follows. Sperm nuclei were incubated in untreated, mock-depleted or Mre11-depleted extracts at 4000 nuclei/µl for 30 min at 22°C and the extract was supplemented with 0.2 U/µl of *EcoRI* and incubated for a further 60 min. The extract was then resuspended in 40 mM HEPES-KOH pH 7.5, 15 mM MgCl₂, 100 mM KCl, 20 mM EDTA and 1% Triton X-100 and incubated on ice for 10 min. The samples were centrifuged at 6000 g for 5 min and the supernatant was collected and labelled with TdT. Briefly, 50 µl of TdT reaction mixture (30 U TdT, TdT reaction buffer and 50 µCi of alpha-³²P-ddATP 10 µCi/µl greater than 3000 Ci/mmol). Reactions were incubated at 37°C overnight. Labelled DNA was purified through G25 gel filtration columns (Amersham). The samples were loaded on 15% Tris-urea acrylamide gels and run for 1 h at 200V. Labelled DNA was transferred to Hybond-N+ membrane (Amersham) for 2 h at 300 V in 1 × TBE buffer. The membrane was then heated at 80°C for 2 h and exposed (Figure 5A and B).

Isolation of DNA oligonucleotide from human cells was obtained as follows: 3×10^7 human U2OS cells arrested by confluence density or synchronized in G1 with 500 μM mimosine (Sigma-Genosys) were irradiated with 10 Gy using a caesium 137 source or mock treated. G1 arrest was monitored with standard protocols using a FACS sorter. The cells were washed with ice-cold PBS once, harvested with a cell scraper in PBS and collected by centrifugation. The cell pellets were then treated for 5 min with lysis buffer (2% sodium dodecyl sulphate, 20 mM EDTA, 20 mM EGTA, 50 mM Tris-HCl, pH 7.5). Tubes were incubated at room temperature for 10 min. Then 25 μl 5 M NaCl was added and tubes were gently inverted three times and stored for 24 h at 4°C. The genomic DNA was then pelleted following centrifugation for 30 min at 9000 g at 4°C. The supernatant was harvested and the small DNA species were extracted with one volume of phenol-chloroform followed by ethanol precipitation overnight at -20°C. DNA was recovered following centrifugation at 9000 g at 4°C for 30 min. DNA was washed once with 70% ethanol and after repeated centrifugation at 9000 g at 4°C for 30 min, the pelleted DNA was resuspended in 50 μl TdT labelling mix (30 U TdT, TdT reaction buffer and 50 μCi of alpha-³²P-ddATP 10 $\mu\text{Ci}/\mu\text{l}$ greater than 3000 Ci/mmol) as per the Fermentas manufacturer's protocol and incubated at 37°C for 30 min. RNase A was then added to the final concentration of 1 mg/ml. The labelling reaction was stopped using 5 μl 0.5 M EDTA. Formamide loading buffer (5 μl) was added to 5 μl of the labelling reaction. The samples were loaded on 15% Tris-urea acrylamide gels and run for 1 h at 200 V. Gels were washed in 35% methanol, 15% acetic acid, wrapped in saran-wrap and immediately exposed.

DNA oligonucleotide injection and immunofluorescence

Human U2OS cell derivatives were cultured in Dulbecco's modified Eagle's medium supplemented with 10% fetal bovine serum. The

cells were grown on poly-L lysine-treated cover slips for at least 48 h in DMED supplemented with 10% FCS prior to manipulations. For microinjections, injection mixtures (10 μl of Alexa Fluor 488 chicken anti-goat IgG (Molecular Probes) plus 5 μl of DNA at 5 $\mu\text{g}/\mu\text{l}$) were loaded onto Femtotip I (Eppendorf) and attached to InjectMan N12 System (Eppendorf) connected to Zeiss Axiovert 200 microscope. The cells were injected into the cytoplasm at ~100–150 hPa injection pressure. For each experiment, about 200 cells were injected and after 30 min cells were fixed in ice-cold 50% methanol-50% acetone mixtures for 10 min on ice. Following fixation, the cells were washed extensively with PBS and incubated for 30 min with blocking solution containing 5% (w/v) non-fat milk in TBST (TBS plus 0.1% Tween-20). The cells were then incubated with mouse anti-ATM pSerine 1981 (Rockland Immunochemicals) overnight in blocking solution. For secondary detection, we used Alexa Fluor 594 chicken anti-mouse IgG (Molecular Probes). The cells were visualized using a Zeiss LSM 510 Confocal microscope.

Supplementary data

Supplementary data are available at *The EMBO Journal* Online (<http://www.embojournal.org>).

Acknowledgements

We thank the members of the Genome Stability Lab for critical discussions, J Gautier for the anti-*Xenopus* ATM serum and T Paull for Mre11, Nbs1 and Rad50 baculoviruses. This study was supported by the Cancer Research UK, the Lister Institute of Preventive Medicine research prize, the EMBO Young Investigator Program and the European Research Council (ERC) start-up grant awarded to VC.

References

- Bakkenist CJ, Kastan MB (2003) DNA damage activates ATM through intermolecular autophosphorylation and dimer dissociation. *Nature* **421**: 499–506
- Barlow JH, Lisby M, Rothstein R (2008) Differential regulation of the cellular response to DNA double-strand breaks in G1. *Mol Cell* **30**: 73–85
- Berkovich E, Monnat Jr RJ, Kastan MB (2007) Roles of ATM and NBS1 in chromatin structure modulation and DNA double-strand break repair. *Nat Cell Biol* **9**: 683–690
- Bhaskara V, Dupre A, Lengsfeld B, Hopkins BB, Chan A, Lee JH, Zhang X, Gautier J, Zakian V, Paull TT (2007) Rad50 adenylate kinase activity regulates DNA tethering by Mre11/Rad50 complexes. *Mol Cell* **25**: 647–661
- Costanzo V, Paull T, Gottesman M, Gautier J (2004a) Mre11 assembles linear DNA fragments into DNA damage signaling complexes. *PLoS Biol* **2**: E110
- Costanzo V, Robertson K, Gautier J (2004b) *Xenopus* cell-free extracts to study the DNA damage response. *Methods Mol Biol* **280**: 213–227
- Costanzo V, Robertson K, Ying CY, Kim E, Avvedimento E, Gottesman M, Grieco D, Gautier J (2000) Reconstitution of an ATM-dependent checkpoint that inhibits chromosomal DNA replication following DNA damage. *Mol Cell* **6**: 649–659
- Crow YJ, Hayward BE, Parmar R, Robins P, Leitch A, Ali M, Black DN, van Bokhoven H, Brunner HG, Hamel BC, Corry PC, Cowan FM, Frints SG, Klepper J, Livingston JH, Lynch SA, Massey RF, Meritet JF, Michaud JL, Ponsot G et al (2006) Mutations in the gene encoding the 3'-5' DNA exonuclease TREX1 cause Aicardi-Goutieres syndrome at the AGS1 locus. *Nat Genet* **38**: 917–920
- D'Amours D, Jackson SP (2001) The yeast Xrs2 complex functions in S phase checkpoint regulation. *Genes Dev* **15**: 2238–2249
- Dupre A, Boyer-Chatenet L, Gautier J (2006) Two-step activation of ATM by DNA and the Mre11-Rad50-Nbs1 complex. *Nat Struct Mol Biol* **13**: 451–457
- Dupre A, Boyer-Chatenet L, Sattler RM, Modi AP, Lee JH, Nicolette ML, Kopelovich L, Jasin M, Baer R, Paull TT, Gautier J (2008) A forward chemical genetic screen reveals an inhibitor of the Mre11-Rad50-Nbs1 complex. *Nat Chem Biol* **4**: 119–125
- Falck J, Coates J, Jackson SP (2005) Conserved modes of recruitment of ATM, ATR and DNA-PKcs to sites of DNA damage. *Nature* **434**: 605–611
- Guo Z, Dunphy WG (2000) Response of *Xenopus* Cds1 in cell-free extracts to DNA templates with double-stranded ends. *Mol Biol Cell* **11**: 1535–1546
- Hickson I, Zhao Y, Richardson CJ, Green SJ, Martin NM, Orr AI, Reaper PM, Jackson SP, Curtin NJ, Smith GC (2004) Identification and characterization of a novel and specific inhibitor of the ataxia-telangiectasia mutated kinase ATM. *Cancer Res* **64**: 9152–9159
- Ira G, Pelliccioli A, Balijja A, Wang X, Fiorani S, Carotenuto W, Liberi G, Bressan D, Wan L, Hollingsworth NM, Haber JE, Foiani M (2004) DNA end resection, homologous recombination and DNA damage checkpoint activation require CDK1. *Nature* **431**: 1011–1017
- Jazayeri A, Falck J, Lukas C, Bartek J, Smith GC, Lukas J, Jackson SP (2006) ATM- and cell cycle-dependent regulation of ATR in response to DNA double-strand breaks. *Nat Cell Biol* **8**: 37–45
- Jenkins TM, Saxena JK, Kumar A, Wilson SH, Ackerman EJ (1992) DNA polymerase beta and DNA synthesis in *Xenopus* oocytes and in a nuclear extract. *Science* **258**: 475–478
- Keogh MC, Kim JA, Downey M, Fillingham J, Chowdhury D, Harrison JC, Onishi M, Datta N, Galicia S, Emili A, Lieberman J, Shen X, Buratowski S, Haber JE, Durocher D, Greenblatt JF, Krogan NJ (2006) A phosphatase complex that dephosphorylates gammaH2AX regulates DNA damage checkpoint recovery. *Nature* **439**: 497–501
- Lee JH, Paull TT (2005) ATM activation by DNA double-strand breaks through the Mre11-Rad50-Nbs1 complex. *Science* **308**: 551–554
- Lee SE, Moore JK, Holmes A, Umez K, Kolodner RD, Haber JE (1998) *Saccharomyces* Ku70, mre11/rad50 and RPA proteins regulate adaptation to G2/M arrest after DNA damage. *Cell* **94**: 399–409
- Mazur DJ, Perrino FW (2001) Excision of 3' termini by the Trex1 and TREX2 3'→5' exonucleases. Characterization of the recombinant proteins. *J Biol Chem* **276**: 17022–17029

- Paull TT, Gellert M (1998) The 3'-5' exonuclease activity of Mre11 facilitates repair of DNA double-strand breaks. *Mol Cell* **1**: 969-979
- Razzell WE, Khorana HG (1959a) Studies on polynucleotides. III. Enzymic degradation; substrate specificity and properties of snake venom phosphodiesterase. *J Biol Chem* **234**: 2105-2113
- Razzell WE, Khorana HG (1959b) Studies on polynucleotides. IV. Enzymic degradation; the stepwise action of venom phosphodiesterase on deoxyribo-oligonucleotides. *J Biol Chem* **234**: 2114-2117
- Richard DJ, Bolderson E, Cubeddu L, Wadsworth RI, Savage K, Sharma GG, Nicolette ML, Tsvetanov S, McIlwraith MJ, Pandita RK, Takeda S, Hay RT, Gautier J, West SC, Paull TT, Pandita TK, White MF, Khanna KK (2008) Single-stranded DNA-binding protein hSSB1 is critical for genomic stability. *Nature* **453**: 677-681
- Sartori AA, Lukas C, Coates J, Mistrik M, Fu S, Bartek J, Baer R, Lukas J, Jackson SP (2007) Human CtIP promotes DNA end resection. *Nature* **450**: 509-514
- Shiloh Y (2006) The ATM-mediated DNA-damage response: taking shape. *Trends Biochem Sci* **31**: 402-410
- Stiff T, Walker SA, Cerosaletti K, Goodarzi AA, Petermann E, Concannon P, O'Driscoll M, Jeggo PA (2006) ATR-dependent phosphorylation and activation of ATM in response to UV treatment or replication fork stalling. *EMBO J* **25**: 5775-5782
- Takeda S, Nakamura K, Taniguchi Y, Paull TT (2007) Ctp1/CtIP and the MRN complex collaborate in the initial steps of homologous recombination. *Mol Cell* **28**: 351-352
- Trenz K, Smith E, Smith S, Costanzo V (2006) ATM and ATR promote Mre11 dependent restart of collapsed replication forks and prevent accumulation of DNA breaks. *EMBO J* **25**: 1764-1774
- Tsukuda T, Fleming AB, Nickoloff JA, Osley MA (2005) Chromatin remodelling at a DNA double-strand break site in *Saccharomyces cerevisiae*. *Nature* **438**: 379-383
- Uziel T, Lerenthal Y, Moyal L, Andegeko Y, Mittelman L, Shiloh Y (2003) Requirement of the MRN complex for ATM activation by DNA damage. *EMBO J* **22**: 5612-5621
- Vaze MB, Pelliccioli A, Lee SE, Ira G, Liberi G, Arbel-Eden A, Foiani M, Haber JE (2002) Recovery from checkpoint-mediated arrest after repair of a double-strand break requires Srs2 helicase. *Mol Cell* **10**: 373-385
- Yang YG, Lindahl T, Barnes DE (2007) Trex1 exonuclease degrades ssDNA to prevent chronic checkpoint activation and autoimmune disease. *Cell* **131**: 873-886
- Yoo HY, Shevchenko A, Dunphy WG (2004) Mcm2 is a direct substrate of ATM and ATR during DNA damage and DNA replication checkpoint responses. *J Biol Chem* **279**: 53353-53364



The EMBO Journal is published by Nature Publishing Group on behalf of European Molecular Biology Organization. This article is licensed under a Creative Commons Attribution-NonCommercial-No Derivative Works 3.0 Licence. [http://creativecommons.org/licenses/by-nc-nd/3.0]